Homogenously isoattenuating insulinoma on biphasic contrast-enhanced computed tomography: Little benefits of diffusion-weighted imaging for lesion detection

ZHENSHAN SHI[1], XIUMEI LI[1], RUIXIONG YOU[1], YUEMING LI[1], XIANYING ZHENG[1], KAMISHA RAMEN[2], VIKASH SAHADEO LOOSA[2], DAIRONG CAO[1] and QUNLIN CHEN[1]

[1]Department of Radiology, First Affiliated Hospital of Fujian Medical University, Fuzhou, Fujian 350005; [2]Department of Radiology, Fujian Medical University, Fuzhou, Fujian 350001, P.R. China

Received December 11, 2017; Accepted May 30, 2018

DOI: 10.3892/ol.2018.9037

Abstract. The aim of the present study was to evaluate the diagnostic benefit of diffusion-weighted imaging (DWI) in the detection of homogenous isoattenuating insulinoma on biphasic contrast-enhanced computed tomography (CT) preoperatively and to determine which magnetic resonance (MR) sequences exhibited the best diagnostic performance. A total of 44 consecutive patients who underwent biphasic contrast-enhanced CT and conventional MR imaging (MRI), including DWI on a 3T scanner, were identified retrospectively. Apparent diffusion coefficient (ADC) values of insulinomas and the surrounding pancreatic parenchyma were compared using a Wilcoxon signed-rank test. Receiver operating characteristic analysis was used to compare the diagnostic accuracy of four randomized image sets [T2-weighted image (WI), axial T1WI, DWI and T2WI + DWI] for each reader. Axial T1-weighted MRI exhibited the highest relative sensitivity for each reader; DWI alone exhibited the lowest relative sensitivity and the lower inter-reader agreement. There was no significant difference in lesion detection between T2WI and T2WI + DWI image sets for each reader. The ADC values of the insulinoma were significantly lower compared with those of the surrounding parenchyma. In conclusion, DWI does not benefit the detection of homogenous isoattenuating insulinoma. Axial T1WI is the optimal pulse sequence. Quantitative assessment of the tumor ADC values may be a useful tool to characterize identified pancreatic neoplasms.

Correspondence to: Dr Dairong Cao or Dr Qunlin Chen, Department of Radiology, First Affiliated Hospital of Fujian Medical University, 20 Cha-Zhong Road, Fuzhou, Fujian 350005, P.R. China
E-mail: 2375530372@qq.com
E-mail: 13960825028@163.com

Abbreviations: CT, computed tomography; MRI, magnetic resonance imaging; DWI, diffusion-weighted imaging; ADC, apparent diffusion coefficient; ICTs, islet cell tumors

Key words: pancreas, diffusion-weighted imaging, magnetic resonance imaging, insulinoma, multi-detector computed tomography

Introduction

Insulinoma is a mostly benign, and solitary pancreatic tumor, with an incidence of 4 cases per 1,000,000 people per year among residents of Olmsted County (MN, USA) for 1927-1986, and it is considered rare (1). Insulinomas often present with hypoglycemic syndromes associated with hormonal hypersecretion and remain the most common functioning neuroendocrine tumors of the pancreas (2). Precise preoperative localization of insulinoma has been shown to be associated with improved cure rates and the prevention of surgical complications (3). However, the detection and localization of the majority of insulinomas are occasionally problematic on multi-detector computed tomography (MDCT) and magnetic resonance imaging (MRI) studies due to their small size and various imaging features (4,5).

Biphasic contrast-enhanced CT and MRI are common non-invasive imaging techniques used to identify the pancreatic neoplasm (6,7). MDCT examination remains the first step in the detection of insulinoma due to its non-invasiveness, widespread availability, and greater spatial and contrast resolution (4,8-11). Typically, the majority of insulinomas are uniformly hyperdense on the arterial phase of biphasic contrast-enhanced CT and markedly hyperintense in the early phase of dynamic contrast-enhanced MRI, which is associated with the hypervascular nature of these tumors (10,12,13). However, certain hypovascular tumors present with an atypical enhancement pattern and appear hypo- or iso-dense relative to the normal pancreatic parenchyma on all phases, and often may not be clearly identified or accurately diagnosed (13-16). Occasionally encountered, small, homogenously isoattenuating insulinoma will be nearly invisible on all but unenhanced MR images due to the absence or subtle change in pancreatic contours, which may not easily be noted (17-19).

In a recent report, Lotfalizadeh *et al* (20) showed that the addition of DWI to morphological and functional MR findings has predictive value for tumor grade of pancreatic

neuroendocrine tumors (pNETs), particularly for quantitative differentiation between G3 and G1-2 tumors (19). DWI may improve the diagnostic performance in depicting and characterizing those small islet cell tumors (ICTs) when added to other conventional MR sequences due to its superior image contrast and functional information provided (21). It has been shown that the monoexponentially-derived apparent diffusion coefficient (ADC) value may be a valuable tool to accurately discriminate between pancreatic cancer and focal mass-like pancreatitis (22,23). However, to the best of our knowledge, the diagnostic value of DWI and which conventional MR sequences show these atypical insulinoma most clearly, remains uncertain. In this sense, the current study presents 22 cases of surgically proven insulinomas, which were homogenously iso-dense relative to the surrounding pancreatic parenchyma on all phases during biphasic CT scanning following intravenous contrast administration preoperatively. The aim of the study was to evaluate if the use of DWI results in a better diagnostic performance for the detection of these atypical insulinomas and to determine which conventional MR sequences show them most definitely.

Patients and methods

Patients. The present retrospective study was approved by the Institutional Review Board of the First Affiliated Hospital of Fujian Medical University (Fuzhou, China), and the requirement for informed consent was waived. The clinical records, and radiological and pathological databases at the First Affiliated Hospital of Fujian Medical University (Fuzhou, China) between January 2010 and March 2017 were reviewed. A total of 44 consecutive patients were identified who underwent biphasic contrast-enhanced CT and conventional MRI, including DWI on a 3T scanner, within 6 weeks of each other for suspected insulinomas. Of the 44 patients who underwent biphasic CT and 3T MR scans, 22 subsequently underwent surgery and were determined to show the presence of insulinoma. Inclusion criteria for this study were as follows: i) Syndromes of hypoglycemia and endogenous hyperinsulinemia were confirmed preoperatively; ii) upper abdominal biphasic contrast-enhanced CT and conventional MR sequences were performed preoperatively; iii) patients with multiple endocrine neoplasia (MEN) syndrome were not included; iv) patients underwent surgery within 4 months of the imaging exams and diagnosis of pNET was confirmed histopathologically; and v) patients experienced symptomatic relief during the course of follow-up. Other causes of hypoglycemia (n=8) with no evidence of insulinomas were excluded, including hepatic insufficiency (n=4), exogenous hyperinsulinism (n=2) and drugs (n=2). In total, 2 patients with a final diagnosis of MEN type 1 (MEN1) syndrome were excluded and 11 patients who underwent surgery at other institutions without a 3.0T MRI machine were excluded. A 79-year-old patient who did not undergo surgery owing to unfitness from comorbidities was also excluded. Overall, 22 patients (13 men and 9 women; age range, 25-60 years; mean age, 46.4 years) with definitive insulinomas according to surgery and histological examination of the resected specimen were evaluated in the study. All 22 patients experienced symptomatic relief following surgery and no recurrence during the follow-up period of 6 months. The diagnosis was no longer that of insulinoma as the patients had been efficiently treated. This final diagnosis was confirmed in all 22 patients either at hospital discharge or during the course of follow-up.

CT protocols. All patients were examined using 320-MDCT scanners (Aquilion ONE; Toshiba Medical Systems, Tokyo, Japan), with the application of the same upper abdominal standardized protocol. Unenhanced and biphasic contrast-enhanced CT that included early arterial and pancreatic parenchymal phases were acquired prior to and following intravenous administration of contrast agent.

Subsequent to the acquisition of unenhanced CT scanning, 300 mg/ml iodine (Ultravist 300; Schering; Bayer Healthcare Pharmaceuticals, Leverkusen, Germany) was injected using a dual-head power injector, through an 18-gauge plastic antecubital catheter. A dose of 1.5 ml/kg of body weight was administered at a rate of 4 ml/sec. The contrast agent administration was followed by an immediate flush of 30 ml normal saline. To determine the timing for pancreatic early arterial and parenchymal phase imaging, a scanning delay was estimated using an automated bolus-tracking technique provided by the manufacturer of the Toshiba CT system. The early arterial phase scanning was performed with a 5-sec delay from aortic enhancement of 250 HU and the pancreatic phase scanning was initiated 45 sec after the contrast agent injection.

MR protocol. Examinations were performed on the same 3.0 T imaging system (Magnetom Trio; Siemens Healthineers, Erlangen, Germany) equipped with an 8-channel phased-array coil centered on the pancreas. The routine MR sequences for the pancreas, including coronal T2-weighted [half-Fourier acquisition single-shot turbo spin echo (TSE)] sequence, axial T1-weighted TSE sequence, axial fat-suppressed T2-weighted TSE sequence, axial T1-weighted in-phase and opposed-phase sequences with echo times of 1.4 and 2.8 msec, respectively, and DWI, were obtained at the Radiology Department of the First Affiliated Hospital of Fujian Medical University.

Axial single-shot echo planar DWI was performed using the following parameters: echo time (TE), 73 msec; repetition time (TR), 6,900 msec; slice thickness, 3 mm; intersection gap, 6 mm; matrix size, 128x128; field of view, 350x350 mm; flip angle, 90˚, parallel imaging reduction factor, 2; partial Fourier factor, 6/8; bandwidth, 2,441 Hz per pixel; and number of excitations, 8 (water excitation with b-value of 50 and 800 sec/mm^2). Axial T1-weighted images (T1WI) were obtained with the following parameters: TR, 670 msec; TE, 14 msec; slice thickness, 3 mm; interslice gap, 6 mm; field of view, 400x280 mm; matrix, 384x188; and number of excitations, 2. DWI and axial T1WI were performed using a normal breathing pattern. The main parameters of the MR sequences are shown in Table I.

ADC maps were automatically created from DW MR images and ADC values were computed on a Syngo workstation (Syngo Multimodality Workplace; Siemens Healthineers). One radiologist, who had knowledge of the precise tumor location on the basis of findings from the overall MRI, surgical and pathological datasets, retrospectively drew the

Table I. Main magnetic resonance imaging parameters.

Sequence	TR/TE, msec	FOV, mm (length/width)	Matrix	Slice thickness/spacing between slices	Pixel band width, KHz	Flip angle, °	Echo train length
Axial fat-suppressed T2-weighted TSE sequence (T2WI)	2999/79	210/380	320x168	5/6	240	140	9
Axial single-shot echo planar imaging (DWI)	6900/73	350/350	128x128	3/6	2441	90	1
Axial T1-weighted images	670/14	400/280	384x188	3/6	279	70	1

TR, repetition time; TE, echo time; DWI, diffusion-weighted imaging; FOV, field of view; WI, weighted-image; TSE, turbo spin echo.

regions of interest (ROIs) (mean ROI size, 0.25 cm^2; range, 0.22-0.28 cm^2) placed within the largest possible tumor area and the surrounding pancreatic parenchyma. ADC values of insulinomas were calculated and compared with ADC values of the surrounding pancreatic parenchyma.

Image analysis. All CT images were retrospectively reviewed by two senior abdominal radiologists (with 18 and 25 years of experience in abdominal MRI, respectively). Two readers had reviewed the surgical and pathological reports and knew the precise location of the tumor. Tumor attenuation values on biphasic CT images were quantitatively calculated and compared with that of the surrounding pancreatic parenchyma. CT attenuation of the tumor (<15 HU) in contrast to the surrounding pancreatic parenchyma in all phases was deemed to represent an isoattenuating tumor (23,24). Tumor enhancement was classified as homogenous, heterogeneous or peripheral on biphasic contrast-enhanced images, and was assessed by two readers. The lesions with homogenously iso-attenuation enhancement patterns were included in the study (Fig. 1).

The MRI assessment of each tumor was divided into four image sets: Axial T1-weighted, T2-weighted, DWI and T2-weighted + DWI. Each set of images was independently interpreted on a digital workstation (Shida PACS system, Fuzhou, China) with the adjustment of window and level freely by two abdominal radiologists (junior reader, with 3 years of experience of abdominal MRI; and senior reader, with 25 years of experience of abdominal MRI). Each reader reviewed the MR images in a randomized, blinded fashion. Two readers independently analyzed the randomly extracted MR images and recorded their findings on a report sheet. The readers knew that the study was being performed to detect insulinomas, but were blinded to any patient information, clinical and biological data, other imaging findings, and surgical and histopathological results. The readers determined the presence or absence of tumor using a 5-point confidence scale as follows: Score 1, definitely absent; score 2, probably absent; score 3, indeterminate; score 4, probably present; and score 5, definitely present. In cases with scores of 4 or 5, a lesion was considered present and the lesion location was carefully recorded. The signal intensity of the tumor was evaluated on four MR image sets compared with that of the surrounding pancreatic parenchyma, and was classified as high, intermediate or low (Figs. 2-4).

Figure 1. Figs. 1-4 depict the same patient with insulinoma. Arterial phase computed tomography representative image revealing a small, well-defined, iso-attenuating mass (arrows) on the anterior periphery of the pancreatic body in a 26-year-old woman.

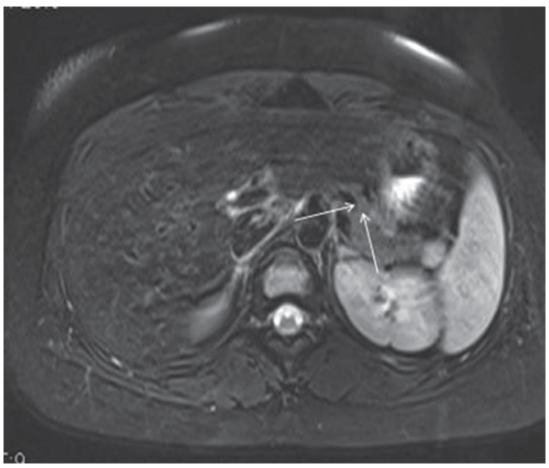

Figure 2. Isointense lesion on a T2-weighted axial magnetic resonance image (arrows).

Statistical analysis. Statistical analysis of all data was performed with SPSS (version 19.0; IBM Corp., Armonk, NY, USA) and MedCalc (MedCalc Software bvba, Ostend, Belgium) software. Quantitative data was determined as the mean ± standard deviation. Descriptive data was shown in

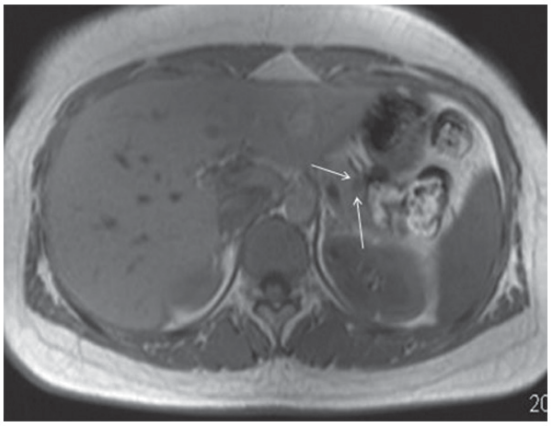

Figure 3. Lesion exhibiting a slow signal on axial T1-weighted images (arrows).

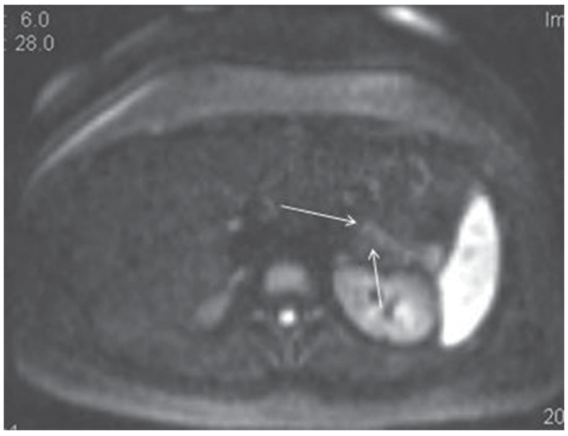

Figure 4. Lesion showing a relatively homogenous, slightly high signal instensity on diffusion-weighted imaging (arrows).

terms of percentages and medians. The Wilcoxon signed-rank test was performed to compare ADC values between the isoattenuating insulinomas and surrounding pancreatic parenchyma of the patients. The Wilcoxon signed-rank test was also performed to compare ADC values between isoattenuating insulinomas and hyperattenuating insulinomas. Prior to receiver operating characteristic (ROC) analysis, κ-values were computed to evaluate inter-observer agreement with interpretation as follows: 0.21-0.40, fair agreement; 0.41-0.60, moderate agreement; 0.61-0.80, good agreement; and 0.81-1.00, excellent agreement (19,25). Friedman's non-parametric test, with multiple comparison between the four image sets was performed with Student-Newman-Keul's post-hoc test, was used to determine the variance of diagnosis confidence level score among four MR image sets for each reader. ROC curve analysis was performed to assess the diagnostic performance of four MR image sets in tumor detection for each reader. The area under the ROC curve (Az) and the 95% confidence interval (CI) of each MR image set was calculated and compared using the paired Student's t-test. Az values (>0.80) were considered to show high diagnostic accuracy, as suggested by a previous study (26). A two-sided P-value of <0.05 was considered to indicate a statistically significant difference.

Results

The median time between later imaging (CT or MR) and surgery was 14 days (range, 3-28 days). The 22 insulinomas confirmed pathologically were solitary and benign. The tumors were distributed throughout the whole pancreas as follows: 3 in the pancreatic head, 11 in the pancreatic body and 8 in the tail. The diameter of these lesions ranged from 9.0 to 18 mm (mean, 14.1 mm). According to the histopathological analysis of the 22 insulinomas, 17 tumors (77%) were classified as G1, 4 (18%) as G2 and 1 (5%) as G3 based on the European Neuroendocrine Tumour Society (ENETS) and the 2010 revised World Health Organization (WHO) recommendations (27,28).

The junior and senior reader detected 20/22 and 21/22 lesions on axial T1WI, 16/22 and 17/22 on axial T2WI, 15/22 and 17/22 on T2WI + DWI, and 4/22 and 8/22 on DWI alone, respectively. Axial T1-weighted MRI had the highest relative sensitivity [20-21/22 (91-95%) lesions] in the detection of insulinoma. Significant differences of the diagnostic confidence level score were found among the four MR image sets for the two readers. The confidence level score of DWI alone was the lowest, while that of axial T1WI was the highest for each reader (Table II).

The weighted κ-values that reflected the diagnosis confidence levels of the readers with regard to image interpretation are summarized in Table III. Good inter-observer agreement was found between the two readers for confirming the presence or absence of lesions on T1WI and T2WI datasets (weighted κ=0.74 and weighted κ=0.87, respectively). Poor inter-observer agreement was found between two readers on DWI and T2WI + DWI image datasets (weighted κ=0.46 and weighted κ=0.53, respectively).

With regard to the use of the ROC curves obtained from the four MR image sets for each reader (Figs. 5 and 6), the relative trends among curves of T2WI + DWI and T2WI were similar, with a highest Az value acquired with axial T1WI. The Az values and 95% CI of each ROC curve for each reader are presented in Table IV. There was no significant difference in the Az values of the four MR image sets between the junior and senior reader, although different numbers of tumors were recorded by the two readers (DWI, P=0.71; T2WI, P=0.89; T2WI + DWI, P=0.42; T1WI, P=0.30). The Az values obtained with axial T1WI were much greater than those of DWI alone for each reader (both P<0.001). The Az values obtained with T2WI + DWI and T2WI were also significantly higher than those of DWI alone for each reader (all P<0.05). The Az values obtained with T1WI were considerably higher than that of T2WI for the junior and senior readers (P=0.04 and P=0.03, respectively). There was no significant difference in the Az values between the T2WI + DWI and T2WI image sets for each reader (P=0.84 and P=0.47, respectively). There was also no statistically significant difference in the Az values between the T1WI and T2WI + DWI image sets for each reader (P=0.12 and P=0.13, respectively).

The mean ADC values ($x10^{-3}$ mm^2/sec) of isoattenuating insulinoma and surrounding pancreatic parenchyma were 1.06±0.58 (range, 0.68-2.46) and 1.23±0.24 (range, 0.78-1.67), respectively. The ADC values of the tumors were consistently higher compared with those of the surrounding pancreatic parenchyma in these patients according to the Wilcoxon signed-rank test (P=0.003; Table V). The mean ADC value

Table II. Friedman-analysis of variance by ranks for the diagnosis confidence level score.

Groups	Junior reader	Senior reader
Axial-T1WI	3.20	3.05
T2WI	2.41	2.41
DWI	1.64	1.82
T2WI + DWI	2.75	2.73
P-value	P=0.0001	P=0.0001

DWI, diffusion-weighted imaging; WI, weighted-image.

Table III. Inter-observer agreement in image interpretation.

Groups	κ-value
Axial-T1WI	0.742
T2WI	0.871
DWI	0.459
T2WI + DWI	0.532

DWI, diffusion-weighted imaging; WI, weighted-image.

Table IV. Az values for ROC analysis and relative sensitivity of fat-suppressed T1WI, T2WI, T2WI + DWI and DWI for tumor detection.

Reader	Az	95% CI	Sensitivity, % (n/total n)
Junior			
Axial-T1WI	0.921±0.04	0.800-0.981	91 (20/22)
T2WI	0.830±0.06	0.686-0.926	68 (15/22)
DWI	0.815±0.07	0.669-0.916	73 (16/22)
T2WI + DWI	0.514±0.09	0.359-0.668	32 (4/22)
Senior			
Axial-T1WI	0.958±0.03	0.850-0.995	95 (21/22)
T2WI	0.820±0.07	0.675-0.920	77 (17/22)
DWI	0.869±0.05	0.733-0.951	77 (17/22)
T2WI + DWI	0.549±0.09	0.391-0.699	36 (8/22)

ROC, receiver operating characteristic; Az, area under the ROC curve; DWI, diffusion-weighted imaging; WI, weighted-image; CI, confidence interval.

of the hyperattenuating insulinomas was 0.81±0.24 (range, 0.53-1.48), but no statistical significance was found between hyperattenuating and isoattenuating insulinomas based on the Wilcoxon signed-rank test (P=0.26). The junior and senior reader detected 16/22 and 17/22 hyperattenuating insulinomas, respectively, on DWI alone. With regard to the use of the ROC curves obtained from isoattenuating and hyperattenuating insulinomas for each reader (Figs. 7 and 8), the Az values

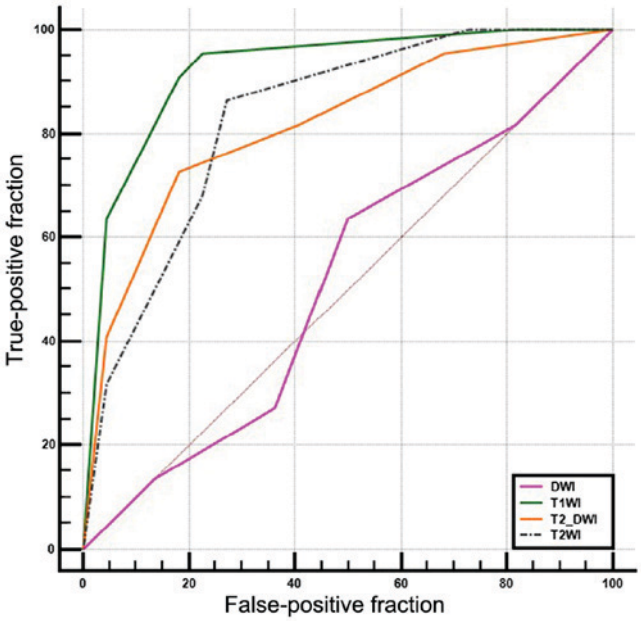

Figure 5. Receiver operating characteristic curves for tumor detection in four magnetic resonance image datasets according to the junior reader. DWI, diffusion-weighted imaging; WI, weighted image.

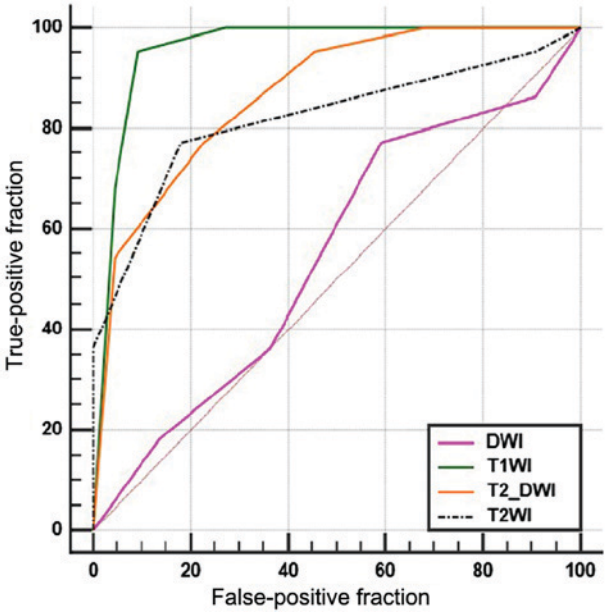

Figure 6. Receiver operating characteristic curves for tumor detection in four magnetic resonance image datasets according to the senior reader. DWI, diffusion-weighted imaging; WI, weighted image.

obtained with the hyperattenuating insulinomas were much greater than those of the isoattenuating tumors for each reader (P=0.027 and P=0.021, respectively).

Discussion

The detection of insulinoma is pivotal in current imaging studies. The ability of various imaging techniques to detect and characterize the pancreatic neoplasms has been studied extensively (5,7,9,28-31). The tumor enhancement pattern of insulinoma allows for an indirect assessment of tumor

Table V. ADC values of insulinoma compared with ADC values of surrounding pancreatic tissue[a].

Insulinoma ADC values (n=22)	Surrounding parenchyma ADC values (n=22)	Wilcoxon signed-rank test	
		Z-value	P-value
Mean	1.06	2.931	0.003
SD	0.58		
Median	0.81		
Minimum	0.68		
Maximum	2.46		

[a]ADC values in insulinoma were lower (1.06±0.58) compared with those in the surrounding pancreatic parenchyma (1.23±0.24). Wilcoxon signed-rank test demonstrated this difference to be statistically significant (P=0.003). ADC, apparent diffusion coefficient; SD, standard deviation.

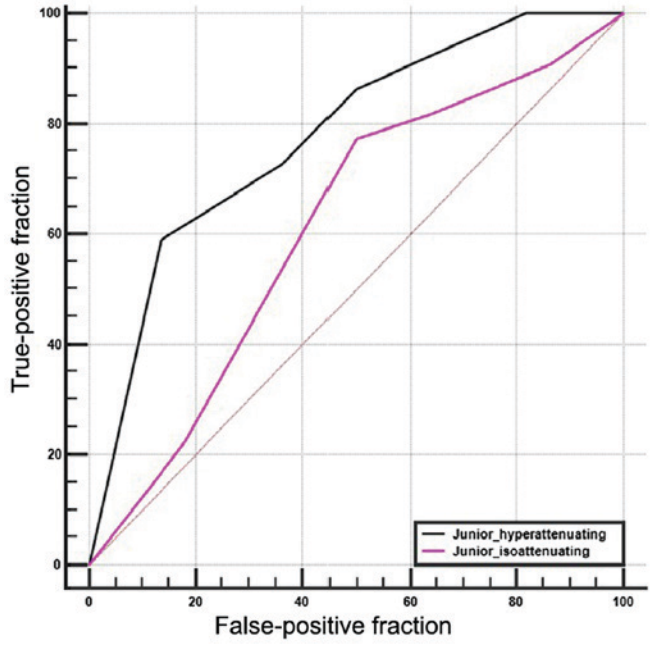

Figure 7. Receiver operating characteristic curves for isoattenuating and hyperattenuating detection with diffusion-weighted imaging alone according to the junior reader.

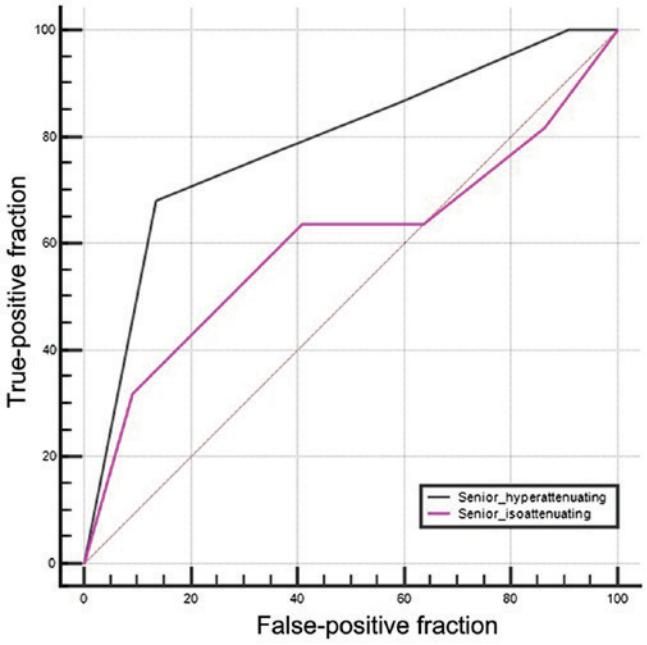

Figure 8. Receiver operating characteristic curves for isoattenuating and hyperattenuating detection with diffusion-weighted imaging alone according to the senior reader.

vascularity, composition and cell density, rather than showing different stages of tumor development (19). Isoattenuating insulinoma on biphasic contrast-enhanced CT, which accounts for 24.9% of all insulinomas (15), poses a diagnostic challenge, even for senior abdominal radiologists, and it has the necessity of referring the patient for MRI examination. The application of DWI and MR cholangiopancreatography improves the diagnostic accuracy of MRI in identifying small insulinomas, and the highest sensitivity for this combined application has been achieved among other non-invasive imaging techniques (10,32-36).

In the present study, the mean tumor size was 14.1 mm and the mean ADC value of the insulinomas was significantly lower than that of the adjacent pancreatic parenchyma, in accordance with previously published data (17,21,37-39). Nevertheless, the mean ADC value (1.06±0.58x10^{-3} mm^2/sec) of tumors in the present study was lower compared with that found in a prior study (1.51±0.35x10^{-3} mm^2/sec) (8), which can probably be explained by the different intrinsic characteristics of the tumors, the higher field strength of the scanner applied (3.0T versus 1.5T) and the presence of smaller nodules (21,39-41).

The present study confirmed the high sensitivity of axial T1WI for the detection of insulinomas (29,42-46), which also provided a contribution to the highest diagnostic confidence of each reader and the highest inter-observer agreement between the two readers, and demonstrated that axial T1WI was the optimal sequence among the four image sets. With a high detection sensitivity of 91 and 95% for the involved junior and senior radiologist, respectively, the present results were superior to that of other studies, with a mean sensitivity of <70% (ranging between 0 and 100%). This was likely due to the small patient cohort and various MR sequences used (10,23,29). The present

results were more likely to be affected by a selection bias: The lesions included in the study showed a homogenous iso-attenuation enhancement pattern on biphasic contrast-enhanced CT, which may imply that the pathology of the insulinoma was dense fibrosis or high tumor cellularity (7,12,15,16,19).

DWI, as part of an upper abdominal conventional MRI protocol, can be utilized to detect lesions with a clinical suspicion of pancreatic ICTs that exhibit negative or indistinct suspicious imaging findings (17,20,39). Nonetheless, the use of DWI in localizing insulinomas remains controversial (17,24,29,32,39,44,47). The present study found that the inter-observer agreement between two readers for determining the presence or absence of tumor on DWI alone image sets was the poorest (weighted κ=0.46). No significant difference in ADC value was observed between the isoattenuating and hyperattenuating insulinomas, whereas hyperattenuating lesions could be detected more easily than the isoattenuating by DWI for each reader based on ROC analysis. The present result tended to similar to that of previous studies (39,44,47), but was inconsistent with several other studies (17,48). A possible explanation for these paradoxical findings is that although DWI is a reliable sequence in the detection of the hypervascular tumors with abundant fluid hyperintense structure, the hypovascular lesions appear slightly hyperintense on DWI and make it extremely difficult to identify. The junior reader and senior reader detected 4 and 8 tumors on DWI image alone, respectively, in the present study, although there was no significant difference in the relative sensitivity between the two readers. This difference was probably as the accuracy of DWI interpretation is dependent on the readers experience to a certain extent. The inter-observer agreement on T2WI was excellent, whereas poor inter-observer agreement on T2WI + DWI was found in the present study. These results are probably explained in part by the unsatisfactory imaging quality at 3.0T for all DWI sequences, which may decrease the diagnostic confidence of readers (particularly for the junior reader), even added to conventional T2WI (49). Moreover, on the basis of ROC analysis, there was no significant difference in the Az values between T2WI + DWI and T2WI for each reader. The present results showed that DWI alone does not benefit the detection of lesions and that it appears to provide a negligible diagnostic contribution to the conventional MRI protocol in the assessment of these atypical tumors.

The present study had several limitations: First, the patient cohort was small. Second, only isoattenuating insulinomas were included in the study. Therefore, there may be a selection bias towards tumor detection. Third, the value of DWI for the prediction of insulinoma grading was not discussed. Further studies are required to confirm this imaging-pathological association using non-invasive image modalities. Last, but equally important, patients with MEN1-associated ICTs were not included since MEN1-associated ICTs may have different DWI signal intensities and ADC values, compared with sporadic insulinomas. Besides, the imaging strategies for MEN1-associated ICTs are also different and further studies are required.

In conclusion, DWI as part of an upper abdominal conventional MRI protocol does not benefit the detection of homogenously isoattenuating insulinomas on biphasic contrast-enhanced CT, despite the significant difference between the tumor and normal surrounding parenchyma upon ADC measurement. Axial T1WI is the optimal pulse sequence in pancreatic homogenously isoattenuating insulinoma detection among conventional MR sequences.

Acknowledgements

Not applicable.

Funding

Funding was received from the Fujian Provincial department of Science and Technology (Grant no. 2016Y0039). The Health and Planning Committee of Fujian Province (Grant no. 2016013). The Fujian Provincial department of Science and Technology (Grant no. 2015J01450) and the Health and Planning Committee of Fujian Province (Grant no. 2017-CX-27).

Availability of data and materials

The datasets used and/or analyzed during the current study are available from the corresponding author on reasonable request.

Authors' contributions

DC designed the present study. ZS wrote the manuscript and DC, QC and YL revised the manuscript. RY, ZS and XL performed the statistical analysis. QC performed imaging analysis. YL conducted MRI scanning procedures. KR and VSL prepared all figures; XZ and ZS performed the region of interest analysis and illustrations. DC performed the imaging analysis. ZS and XL performed MRI scanning.

Ethics approval and consent to participate

The present retrospective study was approved by the Institutional Review Board of the First Affiliated Hospital of Fujian Medical University (Fuzhou, China), and the requirement for informed consent was waived.

Patient consent for publication

The requirement for informed consent was waived by the Institutional Review Board of the First Affiliated Hospital of Fujian Medical University (Fuzhou, China).

Competing interests

The authors declare that they have no competing interests.

References

1. Service FJ, McMahon MM, O'Brien PC and Ballard DJ: Functioning insulinoma-incidence, recurrence, and long-term survival of patients: A 60-year study. Mayo Clin Proc 66: 711-719, 1991.
2. Alessandrino F, Ivanovic AM, Yee EU, Radulovic D, Souza D and Mortele KJ: MDCT and MRI of the ampulla of Vater part I: Technique optimization, normal anatomy, and epithelial neoplasms. Abdom Imaging 40: 3274-3291, 2015.
3. Anaye A, Mathieu A, Closset J, Bali MA, Metens T and Matos C: Successful preoperative localization of a small pancreatic insulinoma by diffusion-weighted MRI. JOP 10: 528-531, 2009.

4. Mehrabi A, Fischer L, Hafezi M, Dirlewanger A, Grenacher L, Diener MK, Fonouni H, Golriz M, Garoussi C, Fard N, *et al*: A systematic review of localization, surgical treatment options, and outcome of insulinoma. Pancreas 43: 675-686, 2014.
5. Bakir B, Salmaslioğlu A, Poyanli A, Rozanes I and Acunas B: Diffusion weighted MR imaging of pancreatic islet cell tumors. Eur J Radiol 74: 214-220, 2010.
6. Barral M, Taouli B, Guiu B, Koh DM, Luciani A, Manfredi R, Vilgrain V, Hoeffel C, Kanematsu M and Soyer P: Diffusion-weighted MR imaging of the pancreas: Current status and recommendations. Radiology 274: 45-63, 2015.
7. Brenner R, Metens T, Bali M, Demetter P and Matos C: Pancreatic neuroendocrine tumor: Added value of fusion of T2-weighted imaging and high b-value diffusion-weighted imaging for tumor detection. Eur J Radiol 81: e746-e749, 2012.
8. Buetow PC, Parrino TV, Buck JL, Pantongrag-Brown L, Ros PR, Dachman AH and Cruess DF: Islet cell tumors of the pancreas: Pathologic-imaging correlation among size, necrosis and cysts, calcification, malignant behavior, and functional status. AJR Am J Roentgenol 165: 1175-1179, 1995.
9. Caramella C, Dromain C, De Baere T, Boulet B, Schlumberger M, Ducreux M and Baudin E: Endocrine pancreatic tumors: Which are the most useful MRI sequences? Eur Radiol 20: 2618-2627, 2010.
10. Metz CE: Some practical issues of experimental design and data analysis in radiological ROC studies. Invest Radiol 24: 234-245, 1989.
11. Buchbender C, Hartung-Knemeyer V, Beiderwellen K, Heusch P, Kühl H, Lauenstein TC, Forsting M, Antoch G and Heusner TA: Diffusion-weighted imaging as part of hybrid PET/MRI protocols for whole-body cancer staging: Does it benefit lesion detection? Eur J Radiol 82: 877-882, 2013.
12. Daneshvar K, Grenacher L, Mehrabi A, Kauczor HU and Hallscheidt P: Preoperative tumor studies using MRI or CT in patients with clinically suspected insulinoma. Pancreatology 11: 487-494, 2011.
13. Dixon E and Pasieka JL: Functioning and nonfunctioning neuroendocrine tumors of the pancreas. Curr Opin Oncol 19: 30-35, 2007.
14. Dromain C and Baudin E: Imaging strategy for staging and follow-up of endocrine tumors. Bull Cancer 93: 1183-1189, 2006 (In French).
15. España-Gómez MN, Velázquez-Fernández D, Bezaury P, Sierra M, Pantoja JP and Herrera MF: Pancreatic insulinoma: A surgical experience. World J Surg 33: 1966-1970, 2009.
16. Fattahi R, Balci NC, Perman WH, Hsueh EC, Alkaade S, Havlioglu N and Burton FR: Pancreatic diffusion-weighted imaging (DWI): Comparison between mass-forming focal pancreatitis (FP), pancreatic cancer (PC), and normal pancreas. J Magn Reson Imaging 29: 350-356, 2009.
17. Fujinaga Y, Lall C, Patel A, Matsushita T, Sanyal R and Kadoya M: MR features of primary and secondary malignant lymphoma of the pancreas: A pictorial review. Insights Imaging 4: 321-329, 2013.
18. Herwick S, Miller FH and Keppke AL: MRI of islet cell tumors of the pancreas. AJR Am J Roentgenol 187: W472-W480, 2006.
19. Hiramoto JS, Feldstein VA, LaBerge JM and Norton JA: Intraoperative ultrasound and preoperative localization detects all occult insulinomas. Arch Surg 136: 1020-1025, 2001.
20. Lotfalizadeh E, Ronot M, Wagner M, Cros J, Couvelard A, Vullierme MP, Allaham W, Hentic O, Ruzniewski P and Vilgrain V: Prediction of pancreatic neuroendocrine tumour grade with MR imaging features: Added value of diffusion-weighted imaging. Eur Radiol 27: 1748-1759, 2017.
21. Ichikawa T, Peterson MS, Federle MP, Baron RL, Haradome H, Kawamori Y, Nawano S and Araki T: Islet cell tumor of the pancreas: Biphasic CT versus MR imaging in tumor detection. Radiology 216: 163-171, 2000.
22. Inan N, Arslan A, Akansel G, Okay E and Gurbuz Y: Unusual magnetic resonance image of an insulinoma with extensive desmoplastic reaction. JOP 9: 61-66, 2008.
23. Kim JH, Park SH, Yu ES, Kim MH, Kim J, Byun JH, Lee SS, Hwang HJ, Hwang JY, Lee SS and Lee MG: Visually isoattenuating pancreatic adenocarcinoma at dynamic-enhanced CT: Frequency, clinical and pathologic characteristics, and diagnosis at imaging examinations. Radiology 257: 87-96, 2010.
24. Zhu L, Xue HD, Sun H, Wang X, He YL, Jin ZY and Zhao YP: Isoattenuating insulinomas at biphasic contrast-enhanced CT: Frequency, clinicopathologic features and perfusion characteristics. Eur Radiol 26: 3697-3705, 2016.
25. Lee EK, Yun TJ, Kim JH, Lee KE, Kim SJ, Won JK, Kang KM, Choi SH and Sohn CH: Effect of tumor volume on the enhancement pattern of parathyroid adenoma on parathyroid four-dimensional CT. Neuroradiology 58: 495-501, 2016.
26. Lee SS, Byun JH, Park BJ, Park SH, Kim N, Park B, Kim JK and Lee MG: Quantitative analysis of diffusion-weighted magnetic resonance imaging of the pancreas: Usefulness in characterizing solid pancreatic masses. J Magn Reson Imaging 28: 928-936, 2008.
27. Klimstra DS, Modlin IR, Coppola D, Lloyd RV and Suster S: The pathologic classification of neuroendocrine tumors: A review of nomenclature, grading, and staging systems. Pancreas 39: 707-712, 2010.
28. Klöppel G, Rindi G, Perren A, Komminoth P and Klimstra DS: The ENETS and AJCC/UICC TNM classifications of the neuroendocrine tumors of the gastrointestinal tract and the pancreas: A statement. Virchows Arch 456: 595-597, 2010.
29. Zhu L, Xue H, Sun H, Wang X, Wu W, Jin Z and Zhao Y: Insulinoma detection with MDCT: Is there a role for whole-pancreas perfusion? AJR Am J Roentgenol 208: 306-314, 2017.
30. Liu Y, Song Q, Jin HT, Lin XZ and Chen KM: The value of multidetector-row CT in the preoperative detection of pancreatic insulinomas. Radiol Med 114: 1232-1238, 2009.
31. Machado MC, da Cunha JE, Jukemura J, Bacchella T, Penteado S, Abdo EE, Machado MA, Herman P, Montagnini AL and Pinotti H: Insulinoma: Diagnostic strategies and surgical treatment. A 22-year experience. Hepatogastroenterology 48: 854-858, 2001.
32. Matsuki M, Inada Y, Nakai G, Tatsugami F, Tanikake M, Narabayashi I, Masuda D, Arisaka Y, Takaori K and Tanigawa N: Diffusion-weighed MR imaging of pancreatic carcinoma. Abdom Imaging 32: 481-483, 2007.
33. Menegaux F, Schmitt G, Mercadier M and Chigot JP: Pancreatic insulinomas. Am J Surg 165: 243-248, 1993.
34. Murakami K, Nawano S, Moriyama N and Onuma Y: Usefulness of magnetic resonance imaging with dynamic contrast enhancement and fat suppression in detecting a pancreatic tumor. Jpn J Clin Oncol 28: 107-111, 1998.
35. Noone TC, Hosey J, Firat Z and Semelka RC: Imaging and localization of islet-cell tumours of the pancreas on CT and MRI. Best Pract Res Clin Endocrinol Metab 19: 195-211, 2005.
36. Ramsay D, Gibson P, Edmunds S and Mendelson R: Pancreatic islet cell tumours presenting as recurrent acute pancreatitis: Imaging features in three cases. Australas Radiol 45: 520-523, 2001.
37. Rha SE, Jung SE, Lee KH, Ku YM, Byun JY and Lee JM: CT and MR imaging findings of endocrine tumor of the pancreas according to WHO classification. Eur J Radiol 62: 371-377, 2007.
38. Sheth S and Fishman EK: Imaging of uncommon tumours of the pancreas. Radiol Clin North Am 40: 1273-1287, 2002.
39. Thoeni RF, Mueller-Lisse UG, Chan R, Do NK and Shyn PB: Detection of small, functional islet cell tumors in the pancreas: Selection of MR imaging sequences for optimal sensitivity. Radiology 214: 483-490, 2000.
40. Toshima F, Inoue D, Komori T, Yoshida K, Yoneda N, Minami T, Matsui O, Ikeda H and Gabata T: Is the combination of MR and CT findings useful in determining the tumor grade of pancreatic neuroendocrine tumors? Jpn J Radiol 35: 242-253, 2017.
41. Wang Y, Chen ZE, Yaghmai V, Nikolaidis P, McCarthy RJ, Merrick L and Miller FH: Diffusion-weighted MR imaging in pancreatic endocrine tumors correlated with histopathologic characteristics. J Magn Reson Imaging 33: 1071-1079, 2011.
42. Wang Y, Miller FH, Chen ZE, Merrick L, Mortele KJ, Hoff FL, Hammond NA, Yaghmai V and Nikolaidis P: Diffusion-weighted MR imaging of solid and cystic lesions of the pancreas. Radiographics 31: E47-E64, 2011.
43. Yao XZ, Yun H, Zeng MS, Wang H, Sun F, Rao SX and Ji Y: Evaluation of ADC measurements among solid pancreatic masses by respiratory-triggered diffusion-weighted MR imaging with inversionrecovery fat-suppression technique at 3.0T. Magn Reson Imaging 31: 524-528, 2013.
44. Ye XH, Gao JY, Yang ZH and Liu Y: Apparent diffusion coefficient reproducibility of the pancreas measured at different MR scanners using diffusion-weighted imaging. J Magn Reson Imaging 40: 1375-1381, 2014.
45. Yoshikawa T, Kawamitsu H, Mitchell DG, Ohno Y, Ku Y, Seo Y, Fujii M and Sugimura K: ADC measurement of abdominal organs and lesions using parallel imaging technique. AJR Am J Roentgenol 187: 1521-1530, 2006.

46. Zhang TP, Zhao YP, Cong L, Liao Q, Dai MH and Guo JC: Noninvasive examinations for localization of insulinoma. Zhonghua Wai Ke Za Zhi 47: 1365-1367, 2009 (In Chinese).
47. Zhao YP, Zhan HX, Zhang TP, Cong L, Dai MH, Liao Q and Cai LX: Surgical management of patients with insulinomas: Result of 292 cases in a single institution. J Surg Oncol 103: 169-174, 2011.
48. Zhu L, Xue H, Sun Z, Li P, Qian T, Xing X, Li N, Zhao Y, Wu W and Jin Z: Prospective comparison of biphasic contrast-enhanced CT, volume perfusion CT, and 3 Tesla MRI with diffusion-weighted imaging for insulinoma detection. J Magn Reson Imaging 46: 1648-1655, 2017.
49. Rosenkrantz AB, Oei M, Babb JS, Niver BE and Taouli B: Diffusion-weighted imaging of the abdomen at 3.0 Tesla: Image quality and apparent diffusion coefficient reproducibility compared with 1.5 Tesla. J Magn Reson Imaging 33: 128-135, 2011.